

Attention Convolutional Binary Neural Tree for Fine-Grained Visual Categorization

Ruyi Ji*, Longyin Wen*, Libo Zhang[†], Dawei Du, Ynajuan Wu, Chen Zhao, Xianglong Liu, Feiyue Huang

Abstract

Fine-grained visual categorization (FGVC) is an important but challenging task due to high intra-class variances and low inter-class variances caused by deformation, occlusion, illumination, etc. An attention convolutional binary neural tree architecture is presented to address those problems for weakly supervised FGVC. Specifically, we incorporate convolutional operations along edges of the tree structure, and use the routing functions in each node to determine the root-to-leaf computational paths within the tree. The final decision is computed as the summation of the predictions from leaf nodes. The deep convolutional operations learn to capture the representations of objects, and the tree structure characterizes the coarse-to-fine hierarchical feature learning process. In addition, we use the attention transformer module to enforce the network to capture discriminative features. The negative log-likelihood loss is used to train the entire network in an end-to-end fashion by SGD with back-propagation. Several experiments on the CUB-200-2011, Stanford Cars and Aircraft datasets demonstrate that the proposed method performs favorably against the state-of-the-arts.

Introduction

Fine-Grained Visual Categorization (FGVC) aims to distinguish subordinate objects categories, such as different species of birds (Wah et al. 2011; Zheng et al. 2017), and flowers (Angelova, Zhu, and Lin 2013). The high intra-class and low inter-class visual variances caused by deformation, occlusion, and illumination, make FGVC to be a highly challenging task. Recently, the FGVC task is quickly dominated by the convolutional neural network (CNN) due to its amazing classification performance. Several algorithms

Ruyi Ji, Libo Zhang, Ynajuan Wu, Chen Zhao are with Institute of Software Chinese Academy of Sciences, Beijing, China. Longyin Wen is with JD Digits, CA USA. Dawei Du is with University at Albany, SUNY, Albany NY, USA. Xianglong Liu is with Beihang University, Beijing China. Feiyue Huang is with Tencent Youtu Lab, Shanghai, China.

[†]Corresponding author: Libo Zhang (libo@iscas.ac.cn). This work is supported by the National Science Foundation of China under Grant No.61807033, and the Key Research Program of Frontier Sciences, CAS, Grant No.ZDBS-LY-JSC038.

*Both authors contributed equally to this research.

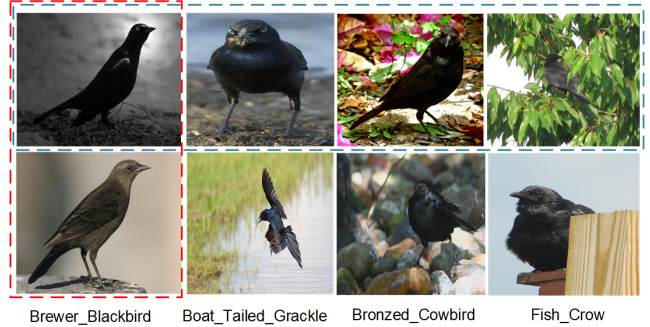


Figure 1: Exemplars of fine-grained visual categorization. FGVC is challenging due to two reasons: (a) high intra-class variances: the birds belonging to the same category usually present significant different appearance, such as illumination variations (the first column), view-point changes (the second column), clutter background (the third column) and occlusion (the forth column); (b) low inter-class variances: the birds in different columns belong to different categories, but share similar appearance in the same rows.

(Lin, Roy Chowdhury, and Maji 2015; Lin et al. 2018) focus on extracting discriminative subtle parts for accurate results. However, the single deep CNN model is hard to describe the differences between subordinate classes, see Figure 1. (Peng, He, and Zhao 2017) present the object-part attention model for FGVC, which uses both object and part attentions to exploit the subtle and local differences to distinguish sub-categories, which demonstrates the effectiveness of using multiple deep models concentrating on different object regions in FGVC.

Inspired by (Tanno et al. 2019), we design an attention convolutional binary neural tree architecture (ACNet) for weakly supervised FGVC, which incorporates convolutional operations along the edges of the tree structure, and use the routing functions in each node to determine the root-to-leaf computational paths within the tree as deep neural networks. This designed architecture makes our method inherits the representation learning ability of the deep convolutional model, and the coarse-to-fine hierarchical feature learning process. In this way, different branches in the tree structure focus on different local object regions for classifi-

cation. The final decision is computed as the summation of the predictions from all leaf nodes. Meanwhile, we use the non-local attention module to enforce the network to capture discriminative features for accurate results. The negative log-likelihood loss is adopted to train the entire network in an end-to-end fashion by stochastic gradient descent (SGD) with back-propagation.

Notably, in contrast to (Tanno et al. 2019) adaptively growing the tree structure in learning process, our method uses a complete binary tree structure with the pre-specified depth, which is data-independent. In addition, the attention transformer module is used to further help our network to achieve better performance. Several experiments are conducted on the CUB-200-2011 (Wah et al. 2011), Stanford Cars (Krause et al. 2013), and Aircraft (Maji et al. 2013) datasets, demonstrating the favorable performance of the proposed method compared to the state-of-the-art methods. We also carried out the ablation study to comprehensively understand the influences of different components in the proposed method. The main contributions of this paper are summarized as follows.

- We present an attention convolutional binary neural tree architecture for FGVC, which incorporates convolutional operations along the edges of the tree structure and use the routing functions in each node to determine the root-to-leaf computational paths within the tree. The final decision is summed over all predictions from leaf nodes.
- The attention transformer module is introduced to enforce the network to capture discriminative features for accurate results.
- Extensive experiments conducted on three challenging dataset, *i.e.*, CUB-200-2011, Stanford Cars, and Aircraft, demonstrate that our method performs favorably against the state-of-the-arts.

Related Works

Deep supervised methods. Some algorithms use object annotations or even dense part/keypoint annotations to guide the training of deep CNN model for FGVC. Zhang *et al.* (Zhang et al. 2014) propose to learn two detectors, *i.e.*, the whole object detector and the part detector, to predict the fine-grained categories based on the pose-normalized representation. Liu *et al.* (Liu et al. 2016) propose a fully convolutional attention networks that glimpses local discriminative regions to adapt to different fine-grained domains. The work in (Huang et al. 2016) construct the part-stacked CNN architecture, which explicitly explains the fine-grained recognition process by modeling subtle differences from object parts. However, these methods rely on labor-intensive part annotations, which limits their applications in real scenarios.

Deep weakly supervised method. To that end, more recent methods only require image-level annotations. Zheng *et al.* (Zheng et al. 2017) introduce a multi-attention CNN model, where part generation and feature learning process reinforce each other for accurate results. Fu *et al.* (Fu, Zheng,

and Mei 2017) develop a recurrent attention module to recursively learn discriminative region attention and region-based feature representation at multiple scales in a mutually reinforced way. Recently, Sun *et al.* (Sun et al. 2018) regulate multiple object parts among different input images by using multiple attention region features of each input image. However, the aforementioned methods merely integrate the attention mechanism in a single network, affecting their performance.

Decision tree. Decision tree is an effective algorithm for classification task. It selects the appropriate directions based on the characteristic of feature. The inherent ability of interpretability makes it as promising direction to pose insight into internal mechanism in deep learning. Xiao (Xiao 2017) propose the principle of fully functioned neural graph and design neural decision tree model for categorization task. Frosst and Hinton (Frosst and Hinton 2017) develop a deep neural decision tree model to understand decision mechanism for particular test case in a learned network. In our work, we integrate the decision tree with neural network to implement sub-branch selection and representation learning simultaneously.

Attention mechanism. Attention mechanism has played an important role in deep learning to mimic human visual mechanism. In (Zagoruyko and Komodakis 2016), the attention is used to make sure the student model focuses on the discriminative regions as teacher model does. (Jetley et al. 2018) propose the cascade attention mechanism on the different layers of CNN and concatenate them to gain discriminative representation as the input of final linear classifier. Hu *et al.* (Hu, Shen, and Sun 2018) apply the attention mechanism from aspect of channels and allocate the different weights according to the contribution of each channel. The CBAM module in (Woo et al. 2018) combines space region attentions with feature map attentions. In contrast to the aforementioned methods, we apply the attention mechanism on each branch of the tree architecture to make the discriminative regions for classification.

Attention Convolutional Binary Neural Tree

Our ACNet model aims to classify each object sample in X to sub-categories, *i.e.*, assign each sample in X with the category label Y , which consists of four modules, *i.e.*, the backbone network, the branch routing, the attention transformer, and the label prediction modules, shown in Figure 2. We define the ACNet as a pair (\mathbb{T}, \mathbb{O}) , where \mathbb{T} defines the topology of the tree, and \mathbb{O} denotes the set of operations along the edges of \mathbb{T} . Notably, we use the full binary tree $\mathbb{T} = \{\mathcal{V}, \mathcal{E}\}$, where $\mathcal{V} = \{v_1, \dots, v_n\}$ is the set of nodes, n is the total number of nodes, and $\mathcal{E} = \{e_1, \dots, e_k\}$ is the set of edges between nodes, k is the total number of edges. Since we use the full binary tree \mathbb{T} , we have $n = 2^h - 1$ and $k = 2^h - 2$, where h is the height of \mathbb{T} . Each node in \mathbb{T} is formed by a routing module determining the sending path of samples, and the attention transformers are used as the operations along the edges.

Meanwhile, we use the asymmetrical architecture in the fully binary tree \mathbb{T} , *i.e.*, two attention transformers are used

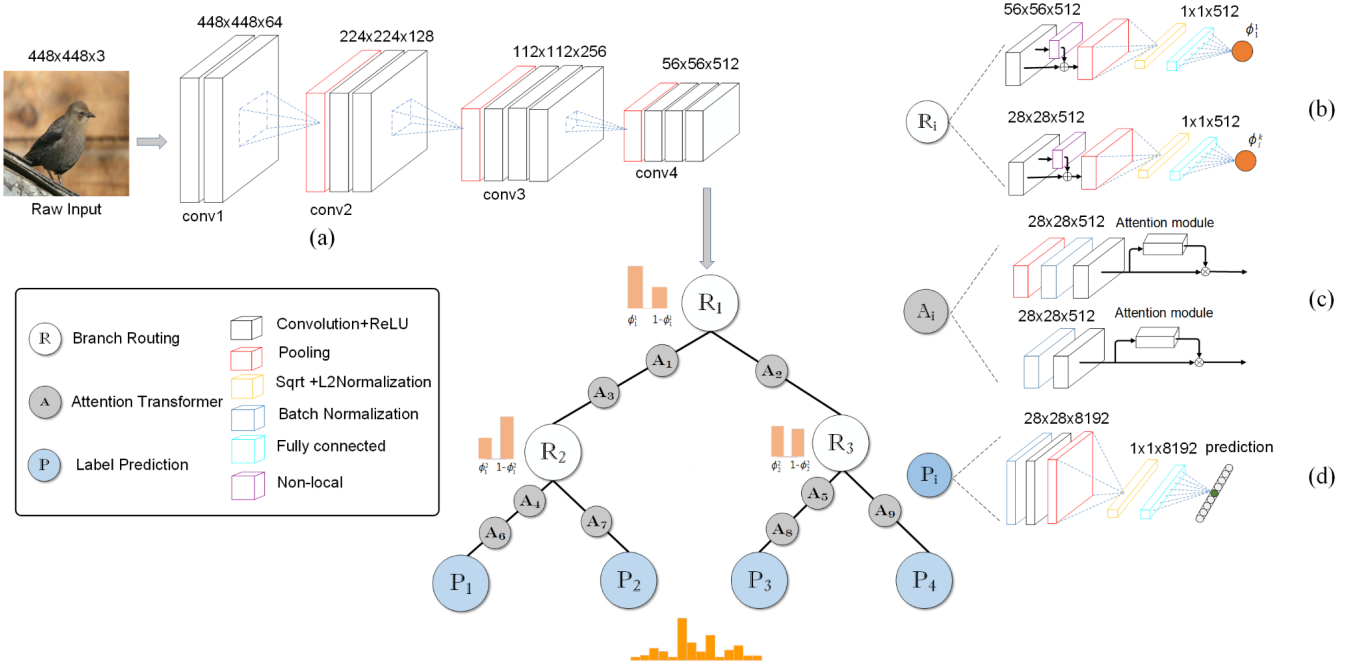


Figure 2: The overview of our ACNet model, formed by (a) the backbone network module, (b) the branch routing module, (c) the attention transformer module, and (d) the label prediction module. Best visualization in color.

in the left edge, and one attention transformer is used in the right edge. In this way, the network is able to capture the different scales of features for accurate results. The detail architecture of our ACNet model is described as follows.

Architecture

Backbone network module. Since the discriminative regions in fine-grained categories are highly localized (Wang, Morariu, and Davis 2018), we need to use a relatively small receptive field of the extracted features by constraining the size and stride of the convolutional filters and pooling kernels. The truncated VGG-16 model (Simonyan and Zisserman 2014) (*i.e.*, retaining the layers from conv1_1 to conv4_3) is used as the backbone network module to extract features, which is pre-trained on the ILSVRC CLS-LOC dataset (Russakovsky et al. 2015). Similar to (Sun et al. 2018), we use the input image size 448×448 instead of the default 224×224 . Notably, ACNet can also work on other pre-trained networks, such as ResNet (He et al. 2016) and Inception V2 (Ioffe and Szegedy 2015).

Branch routing module. As described above, we use the branch routing module to determine which child (*i.e.*, left or right child) the samples would be sent to. Specifically, as shown in Figure 2(b), the i -th routing module $\mathcal{R}_i^k(\cdot)$ at the k -th layer uses one convolutional layer with the kernel size 1×1 , followed by a global context block (Cao et al. 2019). The global context block is an improvement of the simplified non-local (NL) block (Wang et al. 2018) and Squeeze-Excitation (SE) block (Hu, Shen, and Sun 2018), which shares the same implementation with the simplified NL block on the context modeling and fusion steps, and

shares the transform step with the SE block. In this way, the context information is integrated to better describe the objects. After that, we use the global average pooling (Lin, Chen, and Yan 2014), element-wise square-root and L2 normalization (Lin and Maji 2017), and a fully connected layer with the sigmoid activation function to produce a scalar value in $[0, 1]$ indicating the probability of samples being sent to the left or right sub-branches. Let $\phi_i^k(x_j)$ denote the output probability of the j -th sample $x_j \in X$ being sent to the right sub-branch produced by the branch routing module $\mathcal{R}_i^k(x_j)$, where $\phi_i^k(x_j) \in [0, 1]$, $i = 1, \dots, 2^{k-1}$. Thus, we have the probability of the sample $x_j \in X$ being sent to the left sub-branch to be $1 - \phi_i^k(x_j)$. If the probability $\phi_i^k(x_j)$ is larger than 0.5, we prefer the left path instead of the right one; otherwise, the left branch dominates the final decision.

Attention transformer. Inspired by (Hu, Shen, and Sun 2018; Vaswani et al. 2017), we introduce an attention module in the transformers to enforce the network to capture discriminative features, see Figure 3. Specifically, following a convolutional layer with kernel size 3×3 , we insert an attention module, which generates a channel attention map with the size $\mathbb{R}^{C \times 1 \times 1}$ using a batch normalization (BN) layer (Ioffe and Szegedy 2015), a global average pooling (GAP) layer, a fully connected (FC) layer and ReLU activation function, and a fully connected layer and sigmoid function. In this way, the network is guided to focus on meaningful features for accurate results.

Label prediction. For each leaf node in our ACNet model, we use the label prediction module \mathcal{P}_i (*i.e.*, $i = 1, \dots, 2^{h-1}$) to predict the subordinate category of the object x_j , see Figure 2. Let $r_i^k(x_j)$ to be the accumulated

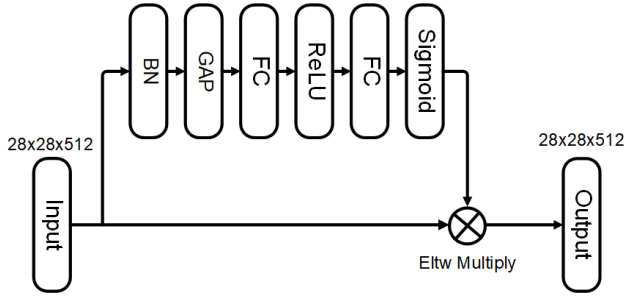


Figure 3: The architecture of the attention transformer module.

probability of the object x_j passing from the root node to the i -th node at the k -th layer. For example, if the root to the node $\mathcal{R}_i^k(\cdot)$ path on the tree is $\mathcal{R}_1^1, \mathcal{R}_1^2, \dots, \mathcal{R}_1^k$, *i.e.*, the object x_j is always sent to the left child, we have $r_i^k(x_j) = \prod_{i=1}^k \phi_1^i(x_j)$. As shown in Figure 2, the label prediction module is formed by a batch normalization layer, a convolutional layer with kernel size 1×1 , a max-pooling layer, a sqrt and L2 normalization layer, and a fully connected layer. Then, the final prediction $\mathcal{C}(x_j)$ of the j -th object x_j is computed as the summation of all leaf predictions multiplied with the accumulated probability generated by the passing branch routing modules, *i.e.*, $\mathcal{C}(x_j) = \sum_{i=1}^{2^{h-1}} \mathcal{P}_i(x_j) r_i^h(x_j)$. We would like to emphasize that $\|\mathcal{C}(x_j)\|_1 = 1$, *i.e.*, the summation of confidences of x_j belonging to all subordinate classes equal to 1,

$$\|\mathcal{C}(x_j)\|_1 = \left\| \sum_{i=1}^{2^{h-1}} \mathcal{P}_i(x_j) r_i^h(x_j) \right\|_1 = 1, \quad (1)$$

where $r_i^h(x_j)$ is the accumulated probability of the i -th node at the leaf layer. We present a short description to prove that $\|\mathcal{C}(x_j)\|_1 = 1$ as follows.

Proof. Let $r_i^k(\cdot)$ be the accumulated probability of the i -th branch routing module $\mathcal{R}_i^k(\cdot)$ at the k -th layer. Thus, the accumulated probabilities of the left and right children corresponding to $\mathcal{R}_i^k(\cdot)$ are $r_{2i-1}^{k+1}(\cdot)$ and $r_{2i}^{k+1}(\cdot)$, respectively. At first, we demonstrate that the summation of the accumulated probabilities $r_{2i-1}^{k+1}(\cdot)$ and $r_{2i}^{k+1}(\cdot)$ is equal to the accumulated probability of their parent $r_i^k(x_j)$. That is,

$$\begin{aligned} & r_{2i-1}^{k+1}(x_j) + r_{2i}^{k+1}(x_j) \\ &= \phi_{2i-1}^{k+1}(x_j) \cdot r_i^k(x_j) + \phi_{2i}^{k+1}(x_j) \cdot r_i^k(x_j) \\ &= \phi_{2i-1}^{k+1}(x_j) \cdot r_i^k(x_j) + (1 - \phi_{2i-1}^{k+1}(x_j)) \cdot r_i^k(x_j) \\ &= (\phi_{2i-1}^{k+1}(x_j) + 1 - \phi_{2i-1}^{k+1}(x_j)) \cdot r_i^k(x_j) \\ &= r_i^k(x_j). \end{aligned} \quad (2)$$

Meanwhile, since we use the fully binary tree \mathbb{T} in our ACNet model, we have

$$\sum_{i=1}^{2^{h-1}} r_i^h(x_j) = \sum_{i=1}^{2^{h-2}} (r_{2i-1}^h(x_j) + r_{2i}^h(x_j)). \quad (3)$$

Based on the above two equations, we can further get

$$\sum_{i=1}^{2^{h-1}} r_i^h(x_j) = \sum_{i=1}^{2^{h-2}} r_i^{h-1}(x_j). \quad (4)$$

This process is carried out iteratively, and we have

$$\sum_{i=1}^{2^{h-1}} r_i^h(x_j) = \dots = r_1^1(x_j) = 1. \quad (5)$$

In addition, since the category prediction $\mathcal{P}_i(x_i)$ is generated by the softmax layer (see Figure 2), we have $\|\mathcal{P}_i(x_j)\|_1 = 1$. Thus,

$$\begin{aligned} \|\mathcal{C}(x_j)\|_1 &= \left\| \sum_{i=1}^{2^{h-1}} \mathcal{P}_i(x_j) r_i^h(x_j) \right\|_1 \\ &= \sum_{i=1}^{2^{h-1}} \|\mathcal{P}_i(x_j)\|_1 r_i^h(x_j) \\ &= \sum_{i=1}^{2^{h-1}} r_i^h(x_j) \\ &= 1. \end{aligned} \quad (6)$$

□

Training

Data augmentation. In the training phase, we use the cropping and flipping operations to augment data to construct a robust model to adapt to variations of objects. That is, we first rescale the original images such that their shorter side is 512 pixels. After that, we randomly crop the patches with the size 448×448 , and randomly flip them to generate the training samples.

Loss function. The loss function for our ACNet is formed by two parts, *i.e.*, the loss for the predictions of leaf nodes, and the loss for the final prediction, computed by the summation over all predictions from the leaf nodes. That is,

$$\mathcal{L} = L(\mathcal{C}(x_j), y^*) + \sum_{i=1}^{2^{h-1}} L(\mathcal{P}_i(x_j), y^*), \quad (7)$$

where h is the height of the tree \mathbb{T} , $L(\mathcal{C}(x_j), y^*)$ is the negative logarithmic likelihood loss of the final prediction $\mathcal{C}(x_j)$ and the ground truth label y^* , and $L(\mathcal{P}_i(x_j), y^*)$ is the negative logarithmic likelihood loss of the i -th leaf prediction and the ground truth label y^* .

Optimization. The backbone network in our ACNet method is pre-trained on the ILSVRC CLS-LOC dataset (Russakovsky et al. 2015). The “xavier” method (Glorot and Bengio 2010) is used to randomly initialize the parameters of the convolutional layers. The entire training process is formed by two stages. For the first stage, the parameters in the truncated VGG-16 network are fixed, and other parameters are trained with 60 epochs. The batch size is set to 24 in training with the initial learning rate 1.0. The learning rate is gradually divided by 4 at the 10-th, 20-th, 30-th, and 40-th epochs. In the second stage, we fine-tune the entire network for 200 epochs. We use the batch size 16 in training with the initial learning rate 0.001. The learning rate is gradually divided by 10 at the 30-th, 40-th, and 50-th epochs. We use the SGD algorithm to train the network with 0.9 momentum, and 0.000005 weight decay in the first stage and 0.0005 weight decay in the second stage.

Experiments

We conduct several experiments on three challenging FGVC datasets, *i.e.*, CUB-200-2011 (Wah et al. 2011), Stanford Cars (Krause et al. 2013), and Aircraft (Maji et al. 2013), to demonstrate the effectiveness of the proposed method. Our method is implemented in the Caffe library (Jia et al. 2014). All the source codes of the proposed method will be made

Method	Anno.	Top-1 Acc. (%)
FCAN (Liu et al. 2016)	✓	84.7
B-CNN (Lin, Roy Chowdhury, and Maji 2015)	✓	85.1
SPDA-CNN (Zhang et al. 2016)	✓	85.1
PN-CNN (Branson et al. 2014)	✓	85.4
STN (Jaderberg et al. 2015)	×	84.1
B-CNN (Lin, Roy Chowdhury, and Maji 2015)	×	84.0
CBP (Gao et al. 2015)	×	84.0
LRB P (Kong and Fowlkes 2016)	×	84.2
FCAN (Liu et al. 2016)	×	84.3
RA-CNN (Fu, Zheng, and Mei 2017)	×	85.3
HIHCA (Cai, Zuo, and Zhang 2017)	×	85.3
Improved B-CNN (Lin and Maji 2017)	×	85.8
BoostCNN (Moghimi et al. 2016)	×	86.2
KP (Cui et al. 2017)	×	86.2
MA-CNN (Zheng et al. 2017)	×	86.5
MAMC (Sun et al. 2018)	×	86.5
MaxEnt (Dubey et al. 2018b)	×	86.5
KERL w/ HR (Chen et al. 2018)	×	87.0
Ours	×	87.6

Table 1: The fine-grained classification results on the CUB-200-2011 dataset.

publicly available after the paper is accepted. All models are trained on a workstation with a 3.26 GHz Intel processor, 512 GB memory, and eight Nvidia V100 GPUs.

CUB-200-2011 Dataset

The Caltech-UCSD birds dataset (CUB-200-2011) (Wah et al. 2011) consists of 11,788 annotated images in 200 subordinate categories, including 5,994 images for training and 5,794 images for testing. The fine-grained classification results are shown in Table 1.

As shown in Table 1, the best supervised method¹, *i.e.* PN-CNN (Branson et al. 2014) using both the object and part level annotations produces 85.4% top-1 accuracy on the CUB-200-2011 dataset. Without part-level annotation, MAMC (Sun et al. 2018) produces 86.5% top-1 accuracy using two attention branches to learn discriminative features in different regions. KERL w/ HR (Chen et al. 2018) designs a single deep gated graph neural network to learn discriminative features, achieving better performance, *i.e.*, 87.0% top-1 accuracy. Compared to the state-of-the-art weakly supervised methods (Chen et al. 2018; Dubey et al. 2018b; Sun et al. 2018), our method achieves the best results with 87.6% top-1 accuracy. This is attributed to the designed attention transformer module and the coarse-to-fine hierarchical feature learning process.

¹Notably, the supervised method requires object or part level annotations, demanding significant human effort. Thus, most of recent methods focus on the weakly supervised methods, pushing the state-of-the-art weakly supervised methods surpassing the performance of previous supervised methods.

Method	Anno.	Top-1 Acc. (%)
FCAN (Liu et al. 2016)	✓	91.3
PA-CNN (Krause et al. 2015)	✓	92.6
FCAN (Liu et al. 2016)	×	89.1
B-CNN (Lin, Roy Chowdhury, and Maji 2015)	×	90.6
LRBP (Kong and Fowlkes 2016)	×	90.9
RAN (Wang et al. 2017)	×	91.0
HIHCA (Cai, Zuo, and Zhang 2017)	×	91.7
Improved B-CNN (Lin and Maji 2017)	×	92.0
BoostCNN (Moghimi et al. 2016)	×	92.1
KP (Cui et al. 2017)	×	92.4
RA-CNN (Fu, Zheng, and Mei 2017)	×	92.5
MA-CNN (Zheng et al. 2017)	×	92.8
MAMC (Sun et al. 2018)	×	93.0
MaxEnt (Dubey et al. 2018b)	×	93.0
WS-DAN (Hu and Qi 2019)	×	93.0
Ours	×	93.5

Table 2: The fine-grained classification results on the Stanford Cars dataset.

Stanford Cars Dataset

The Stanford Cars dataset (Krause et al. 2013) contains 16,185 images from 196 classes, which is formed by 8,144 images for training and 8,041 images for testing. The subordinate categories are determined by the *Make*, *Model*, and *Year* of cars.

As shown in Table 2, previous methods using part-level annotations (*i.e.*, FCAN (Liu et al. 2016) and PA-CNN (Krause et al. 2015)) only produces less than 93.0% top-1 accuracy. The recent weakly supervised method WS-DAN (Hu and Qi 2019) designs the attention-guided data augmentation strategy to exploit discriminative object parts, achieving 93.0% top-1 accuracy. Without using any fancy data augmentation strategy, our method achieves the best top-1 accuracy, *i.e.*, 93.5%.

Aircraft Dataset

The Aircraft dataset (Maji et al. 2013) is a fine-grained dataset of 100 different aircraft variants formed by 10,000 annotated images, which is divided into two subsets, *i.e.*, the training set with 6,667 images and the testing set with 3,333 images. Specifically, the category labels are determined by the *Model*, *Variant*, *Family* and *Manufacturer* of airplanes. The evaluation results are presented in Table 3.

As shown in Table 3, our model performs on par with the state-of-the-art method MA-CNN (Zheng et al. 2017), *i.e.*, 90.4% vs. 89.9% top-1 accuracy. The operations along different root-to-leaf paths in our tree architecture \mathbb{T} focus on exploiting discriminative features on different object regions, which help each other to achieve the best performance in FGVC.

Ablation Study

We conduct several ablation experiments to study the influence of some important parameters and different components of our ACNet method on the CUB-200-2011 dataset.

Method	Anno.	Top-1 Acc. (%)
MG-CNN (Wang et al. 2015)	✓	86.6
MDTP (Wang et al. 2016)	✓	88.4
RA-CNN (Fu, Zheng, and Mei 2017)	×	88.2
MA-CNN (Zheng et al. 2017)	×	89.9
B-CNN (Lin, Roy Chowdhury, and Maji 2015)	×	86.9
KP (Cui et al. 2017)	×	86.9
LRBP (Kong and Fowlkes 2016)	×	87.3
HIHCA (Cai, Zuo, and Zhang 2017)	×	88.3
Improved B-CNN (Lin and Maji 2017)	×	88.5
BoostCNN (Moghimani et al. 2016)	×	88.5
PC-DenseNet-161 (Dubey et al. 2018a)	×	89.2
MaxEnt (Dubey et al. 2018b)	×	89.8
MA-CNN (Zheng et al. 2017)	×	89.9
Ours	×	90.4

Table 3: The fine-grained classification results on the Aircraft dataset.

Height of the Tree	Top-1 Acc. (%)
1	82.2
2	86.0
3	87.6
4	85.5

Table 4: Effect of the height of the tree \mathbb{T} on the CUB-200-2011 dataset.

Effectiveness of the tree architecture \mathbb{T} . To validate the effectiveness of the tree architecture design, we construct two variants, *i.e.*, VGG and w/ Tree, of our ACNet method. Specifically, we construct the VGG method by only using the VGG-16 backbone network for classification, and further integrate the tree architecture to form the w/ Tree method. The evaluation results are reported in Figure 5. As shown in Figure 5, we find that using the tree architecture significantly improves the accuracy, *i.e.*, 3.5% improvements in top-1 accuracy, which demonstrates the effectiveness of the designed tree architecture \mathbb{T} in our ACNet method.

In addition, we also use the Grad-CAM method (Selvaraju et al. 2017) to generate the heatmaps to visualize the responses of the leaf nodes in our ACNet model on the CUB-200-2011 dataset in Figure 4. As shown in Figure 4, we observe that different leaf nodes concentrate on different regions of images. For example, the leaf node corresponding to the first column focuses more on the background region, the leaf node corresponding to the second column focuses more on the head region, and the other two leaf nodes are more interested in the patches of wings and tail. The different leaf nodes help each other to construct more effective model for accurate results.

Height of the tree \mathbb{T} . To explore the effect of the height of the tree \mathbb{T} , we construct four variants with different heights of tree in Table 4. Notably, the tree \mathbb{T} is degenerated to a single node when the height of the tree is set to 1, *i.e.*, only the backbone VGG-16 network is used in classification. As

Mode	Level	Leaf Node	Top-1 Acc. (%)
symmetry	3	4	86.2
asymmetry	3	4	87.6

Table 5: Effectiveness of the asymmetrical architecture of the tree \mathbb{T} on the CUB-200-2011 dataset.

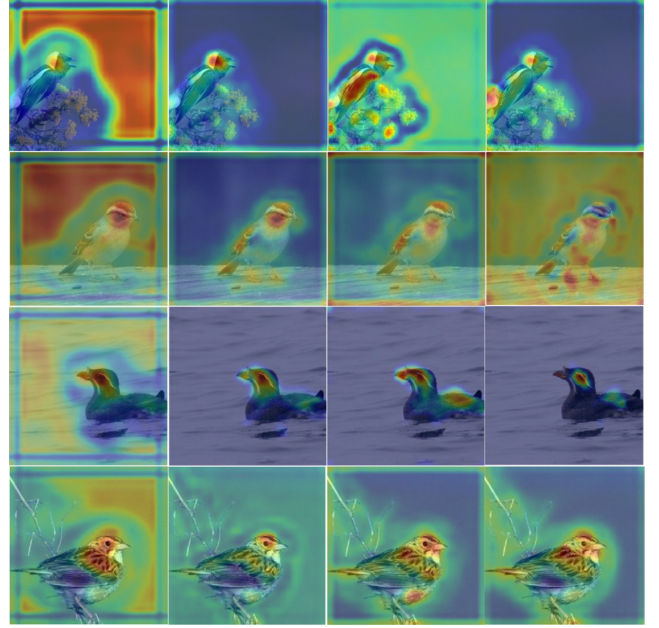


Figure 4: Visualization of the responses in different leaf nodes in our ACNet method. Each column presents a response heatmap of each leaf node.

shown in Table 4, we find that our ACNet achieves the best performance (*i.e.*, 87.6% top-1 accuracy) with the height of tree equals to 3, *i.e.*, $h = 3$. If we set $h \leq 2$, there are limited number of parameters in our ACNet model, which are not enough to represent the significant variations of the subordinate categories. However, if we set $h = 4$, too many parameters with limited number of training data cause overfitting of our ACNet model, which greatly affects the performance.

Asymmetrical architecture of the tree \mathbb{T} . To validate the effectiveness of the asymmetrical architecture design in \mathbb{T} , we construct two variants, *i.e.*, one uses the symmetry architecture, and another one uses the asymmetrical architecture, and set the height of the tree \mathbb{T} to be 3. The evaluation results are reported in Table 5. As shown in Table 5, we find that the proposed method produces 86.2% top-1 accuracy using the symmetrical architecture. If we use the asymmetrical architecture, the top-1 accuracy is improved 1.4% to 87.6%. We speculate that the asymmetrical architecture is able to fuse various features with different receptive fields for better performance.

Effectiveness of the attention transformer module. We construct a variant “w/ Tree-Attn”, of the proposed ACNet model, to validate the effectiveness of the attention transformer module in Figure 5. Specifically, we add the atten-

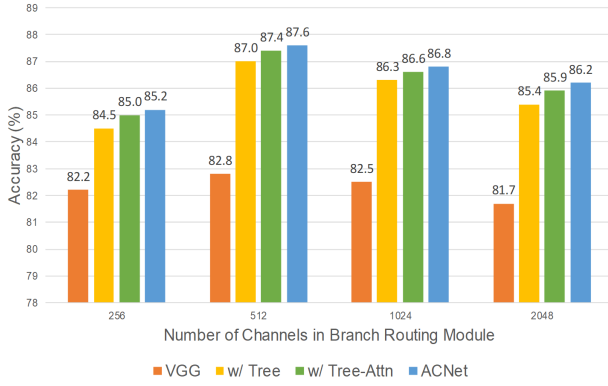


Figure 5: Effect of the various components in the proposed ACNet method on the CUB-200-2011 dataset.

Pooling	Top-1 Acc. (%)
GMP	87.2
GAP	87.6

Table 6: The comparison results of using GMP and GAP in the branch routing module on the CUB-200-2011 dataset.

tion block in the transformer module in the w/ Tree method to construct the “w/ Tree-Attn” method. As shown in Figure 5, the “w/ Tree-Attn” method performs consistently better than the “w/ Tree” method, producing higher top-1 accuracy with different number of channels, *i.e.*, improving 0.425% top-1 accuracy in average, which demonstrate that the attention mechanism is effective for fine-grained classification.

Components in the branch routing module. We analyze the effectiveness of the global context block (Cao et al. 2019) in the branch routing module in Figure 5. As shown in Figure 5, we find that our ACNet method produces the best results with different number of channels in the branch routing module. After removing the global context block, the top-1 accuracy drops 0.225% in average, which demonstrate that the global context block (Cao et al. 2019) is useful to improve the accuracy of the fine-grained classification.

Meanwhile, we also study the effectiveness of the pooling strategy in the branch routing module in Table 6. As shown in Table 6, we observe that using the global max-pooling (GMP) instead of the global average pooling (GAP) leads to 0.4% top-1 accuracy drop on the CUB-200-2011 dataset. We speculate that the GAP operation encourages the filter to focus on high average response regions instead of the only maximal ones, which is able to integrate more context information for better performance.

In addition, we use the Grad-CAM method (Selvaraju et al. 2017) to visualize the focuses of different branch routing modules (*i.e.*, the R_1 , R_2 and R_3 modules in Figure 2) in Figure 6. As shown in Figure 6, we find that different branch routing modules focus on different discriminative regions. For example, the feature maps of the R_1 module pay more attentions to the whole bird region, while the feature maps of the R_2 and R_3 module focus more on the wings and

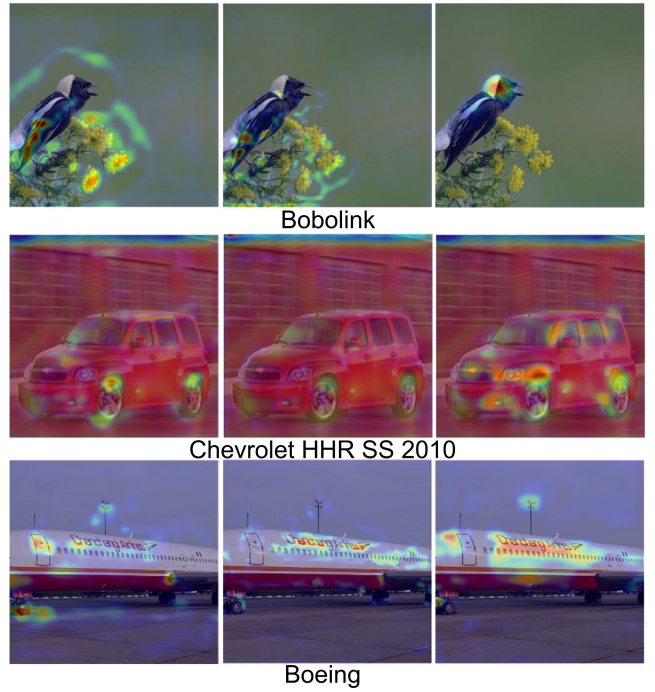


Figure 6: Visualization of the responses in different branch routing modules.

head regions of the bird, see the example *Bobolink* in the first row of Figure 6. This phenomenon demonstrates that our hierarchical feature extraction process in the tree \mathbb{T} architecture gradually enforces our model to focus on more discriminative detail regions of object.

Conclusion

In this paper, we present an attention convolutional binary neural tree for weakly supervised FGVC, which incorporates convolutional operations along edges of the tree structure, and uses the routing functions in each node to determine the root-to-leaf computational paths within the tree. The final decision is produced by max-voting the predictions from leaf nodes. To enforce the network to capture discriminative features for accurate results, we insert the attention transformer module into the convolutional operations along edges. The entire network is trained in an end-to-end fashion by the SGD optimization method with negative log-likelihood loss. Extensive experiments are conducted on three challenging datasets, *i.e.*, CUB-200-2011, Stanford Cars, and Aircraft, demonstrating the favorable performance of the proposed method against the state-of-the-arts.

References

- [Angelova, Zhu, and Lin 2013] Angelova, A.; Zhu, S.; and Lin, Y. 2013. Image segmentation for large-scale subcategory flower recognition. In *WACV*, 39–45.
- [Branson et al. 2014] Branson, S.; Horn, G. V.; Belongie, S. J.; and Perona, P. 2014. Bird species categorization using pose normalized deep convolutional nets. *CoRR* abs/1406.2952.

- [Cai, Zuo, and Zhang 2017] Cai, S.; Zuo, W.; and Zhang, L. 2017. Higher-order integration of hierarchical convolutional activations for fine-grained visual categorization. In *ICCV*, 511–520.
- [Cao et al. 2019] Cao, Y.; Xu, J.; Lin, S.; Wei, F.; and Hu, H. 2019. Gcnet: Non-local networks meet squeeze-excitation networks and beyond. *CoRR* abs/1904.11492.
- [Chen et al. 2018] Chen, T.; Lin, L.; Chen, R.; Wu, Y.; and Luo, X. 2018. Knowledge-embedded representation learning for fine-grained image recognition. In *IJCAI*, 627–634.
- [Cui et al. 2017] Cui, Y.; Zhou, F.; Wang, J.; Liu, X.; Lin, Y.; and Belongie, S. J. 2017. Kernel pooling for convolutional neural networks. In *CVPR*, 3049–3058.
- [Dubey et al. 2018a] Dubey, A.; Gupta, O.; Guo, P.; Raskar, R.; Farrell, R.; and Naik, N. 2018a. Pairwise confusion for fine-grained visual classification. In *ECCV*, 71–88.
- [Dubey et al. 2018b] Dubey, A.; Gupta, O.; Raskar, R.; and Naik, N. 2018b. Maximum-entropy fine grained classification. In *NeurIPS*, 635–645.
- [Frosst and Hinton 2017] Frosst, N., and Hinton, G. E. 2017. Distilling a neural network into a soft decision tree. *CoRR* abs/1711.09784.
- [Fu, Zheng, and Mei 2017] Fu, J.; Zheng, H.; and Mei, T. 2017. Look closer to see better: Recurrent attention convolutional neural network for fine-grained image recognition. In *CVPR*, 4476–4484.
- [Gao et al. 2015] Gao, Y.; Beijbom, O.; Zhang, N.; and Darrell, T. 2015. Compact bilinear pooling. *CoRR* abs/1511.06062.
- [Glorot and Bengio 2010] Glorot, X., and Bengio, Y. 2010. Understanding the difficulty of training deep feedforward neural networks. In *AISTATS*, 249–256.
- [He et al. 2016] He, K.; Zhang, X.; Ren, S.; and Sun, J. 2016. Deep residual learning for image recognition. In *CVPR*, 770–778.
- [Hu and Qi 2019] Hu, T., and Qi, H. 2019. See better before looking closer: Weakly supervised data augmentation network for fine-grained visual classification. *CoRR* abs/1901.09891.
- [Hu, Shen, and Sun 2018] Hu, J.; Shen, L.; and Sun, G. 2018. Squeeze-and-excitation networks. In *CVPR*, 7132–7141.
- [Huang et al. 2016] Huang, S.; Xu, Z.; Tao, D.; and Zhang, Y. 2016. Part-stacked CNN for fine-grained visual categorization. In *CVPR*, 1173–1182.
- [Ioffe and Szegedy 2015] Ioffe, S., and Szegedy, C. 2015. Batch normalization: Accelerating deep network training by reducing internal covariate shift. In *ICML*, 448–456.
- [Jaderberg et al. 2015] Jaderberg, M.; Simonyan, K.; Zisserman, A.; and Kavukcuoglu, K. 2015. Spatial transformer networks. In *NeurIPS*, 2017–2025.
- [Jetley et al. 2018] Jetley, S.; Lord, N. A.; Lee, N.; and Torr, P. H. S. 2018. Learn to pay attention. *CoRR* abs/1804.02391.
- [Jia et al. 2014] Jia, Y.; Shelhamer, E.; Donahue, J.; Karayev, S.; Long, J.; Girshick, R. B.; Guadarrama, S.; and Darrell, T. 2014. Caffe: Convolutional architecture for fast feature embedding. *CoRR* abs/1408.5093.
- [Kong and Fowlkes 2016] Kong, S., and Fowlkes, C. C. 2016. Low-rank bilinear pooling for fine-grained classification. *CoRR* abs/1611.05109.
- [Krause et al. 2013] Krause, J.; Stark, M.; Deng, J.; and Fei-Fei, L. 2013. 3d object representations for fine-grained categorization. In *ICCVW*, 554–561.
- [Krause et al. 2015] Krause, J.; Jin, H.; Yang, J.; and Li, F. 2015. Fine-grained recognition without part annotations. In *CVPR*, 5546–5555.
- [Lin and Maji 2017] Lin, T., and Maji, S. 2017. Improved bilinear pooling with cnns. In *BMVC*.
- [Lin et al. 2018] Lin, H.; Hu, Y.; Chen, S.; Yao, J.; and Zhang, L. 2018. Fine-grained classification of cervical cells using morphological and appearance based convolutional neural networks. *CoRR* abs/1810.06058.
- [Lin, Chen, and Yan 2014] Lin, M.; Chen, Q.; and Yan, S. 2014. Network in network. In *ICLR*.
- [Lin, Roy Chowdhury, and Maji 2015] Lin, T.; Roy Chowdhury, A.; and Maji, S. 2015. Bilinear CNN models for fine-grained visual recognition. In *ICCV*, 1449–1457.
- [Liu et al. 2016] Liu, X.; Xia, T.; Wang, J.; and Lin, Y. 2016. Fully convolutional attention localization networks: Efficient attention localization for fine-grained recognition. *CoRR* abs/1603.06765.
- [Maji et al. 2013] Maji, S.; Rahtu, E.; Kannala, J.; Blaschko, M. B.; and Vedaldi, A. 2013. Fine-grained visual classification of aircraft. *CoRR* abs/1306.5151.
- [Moghimani et al. 2016] Moghimani, M.; Belongie, S. J.; Saberian, M. J.; Yang, J.; Vasconcelos, N.; and Li, L. 2016. Boosted convolutional neural networks. In *BMVC*.
- [Peng, He, and Zhao 2017] Peng, Y.; He, X.; and Zhao, J. 2017. Object-part attention driven discriminative localization for fine-grained image classification. *CoRR* abs/1704.01740.
- [Russakovsky et al. 2015] Russakovsky, O.; Deng, J.; Su, H.; Krause, J.; Satheesh, S.; Ma, S.; Huang, Z.; Karpathy, A.; Khosla, A.; Bernstein, M. S.; Berg, A. C.; and Li, F. 2015. Imagenet large scale visual recognition challenge. *IJCV* 115(3):211–252.
- [Selvaraju et al. 2017] Selvaraju, R. R.; Cogswell, M.; Das, A.; Vedantam, R.; Parikh, D.; and Batra, D. 2017. Grad-cam: Visual explanations from deep networks via gradient-based localization. In *ICCV*, 618–626.
- [Simonyan and Zisserman 2014] Simonyan, K., and Zisserman, A. 2014. Very deep convolutional networks for large-scale image recognition. *CoRR* abs/1409.1556.
- [Sun et al. 2018] Sun, M.; Yuan, Y.; Zhou, F.; and Ding, E. 2018. Multi-attention multi-class constraint for fine-grained image recognition. In *ECCV*, 834–850.
- [Tanno et al. 2019] Tanno, R.; Arulkumaran, K.; Alexander, D. C.; Criminisi, A.; and Nori, A. V. 2019. Adaptive neural trees. In *ICML*, 6166–6175.
- [Vaswani et al. 2017] Vaswani, A.; Shazeer, N.; Parmar, N.; Uszkoreit, J.; Jones, L.; Gomez, A. N.; Kaiser, L.; and Polosukhin, I. 2017. Attention is all you need. In *NeurIPS*, 5998–6008.
- [Wah et al. 2011] Wah, C.; Branson, S.; Welinder, P.; Perona, P.; and Belongie, S. 2011. The Caltech-UCSD Birds-200-2011 Dataset. Technical report, California Institute of Technology.
- [Wang et al. 2015] Wang, D.; Shen, Z.; Shao, J.; Zhang, W.; Xue, X.; and Zhang, Z. 2015. Multiple granularity descriptors for fine-grained categorization. In *ICCV*, 2399–2406.
- [Wang et al. 2016] Wang, Y.; Choi, J.; Morariu, V. I.; and Davis, L. S. 2016. Mining discriminative triplets of patches for fine-grained classification. *CoRR* abs/1605.01130.
- [Wang et al. 2017] Wang, F.; Jiang, M.; Qian, C.; Yang, S.; Li, C.; Zhang, H.; Wang, X.; and Tang, X. 2017. Residual attention network for image classification. In *CVPR*, 6450–6458.
- [Wang et al. 2018] Wang, X.; Girshick, R. B.; Gupta, A.; and He, K. 2018. Non-local neural networks. In *CVPR*, 7794–7803.
- [Wang, Morariu, and Davis 2018] Wang, Y.; Morariu, V. I.; and Davis, L. S. 2018. Learning a discriminative filter bank within a CNN for fine-grained recognition. In *CVPR*, 4148–4157.

- [Woo et al. 2018] Woo, S.; Park, J.; Lee, J.; and Kweon, I. S. 2018. CBAM: convolutional block attention module. *CoRR* abs/1807.06521.
- [Xiao 2017] Xiao, H. 2017. NDT: neural decision tree towards fully functioned neural graph. *CoRR* abs/1712.05934.
- [Zagoruyko and Komodakis 2016] Zagoruyko, S., and Komodakis, N. 2016. Paying more attention to attention: Improving the performance of convolutional neural networks via attention transfer. *CoRR* abs/1612.03928.
- [Zhang et al. 2014] Zhang, N.; Donahue, J.; Girshick, R. B.; and Darrell, T. 2014. Part-based r-cnns for fine-grained category detection. In *ECCV*, 834–849.
- [Zhang et al. 2016] Zhang, H.; Xu, T.; Elhoseiny, M.; Huang, X.; Zhang, S.; Elgammal, A. M.; and Metaxas, D. N. 2016. SPDA-CNN: unifying semantic part detection and abstraction for fine-grained recognition. In *CVPR*, 1143–1152.
- [Zheng et al. 2017] Zheng, H.; Fu, J.; Mei, T.; and Luo, J. 2017. Learning multi-attention convolutional neural network for fine-grained image recognition. In *ICCV*, 5219–5227.